Genetic structure, ecological versatility, and skull shape differentiation in Arvicola water voles (Rodentia, Cricetidae)

Pascale Chevret, Sabrina Renaud, Zeycan Helvaci, Rainer Ulrich, Jean-pierre Quéré, Johan Michaux

Genetic structure, ecological versatility, and skull shape differentiation in *Arvicola* water voles (Rodentia, Cricetidae)

Short running title: *Arvicola* phylogeography and morphometry

Pascale Chevret [1], Sabrina Renaud [1], Zeycan Helvaci [2,3], Rainer Ulrich [4], Jean-Pierre Quéré [5], Johan R. Michaux [2, 6]

[1] Laboratoire de Biométrie et Biologie Evolutive, UMR 5558, CNRS, Université Claude Bernard Lyon 1, Université de Lyon, Villeurbanne, France

[2] Conservation Genetics Laboratory, Institut de Botanique, Chemin de la Vallée, 4, 4000 Liège, Belgium

[3] Present address: Aksaray Üniversitesi Fen Edebiyat Fakültesi, 68100 Merkez/ Aksaray, Turkey

[4] Institute of Novel and Emerging Infectious Diseases, Friedrich-Loeffler-Institut, Federal Research Institute for Animal Health, Südufer 10, 17493 Greifswald - Insel Riems, Germany

[5] Centre de Biologie et Gestion des Populations (INRA / IRD / Cirad /Montpellier SupAgro), Campus international de Baillarguet, CS 30016, F-34988, Montferrier-sur-Lez Cedex, France

[6] CIRAD/INRA UMR117 ASTRE, Campus International de Baillarguet, 34398 Montpellier Cedex 5, France

Corresponding author: Pascale Chevret, e-mail: pascale.chevret@univ-lyon1.fr

Keywords: Phylogeography, geometric morphometrics, cytochrome *b*, *Arvicola amphibius*, plasticity

Abstract

Water voles from the genus *Arvicola* display an amazing ecological versality, with aquatic and fossorial populations. The Southern water vole (*A. sapidus*) is largely accepted as a valid species, as well as the newly described *A. persicus*. In contrast, the taxonomic status and evolutionary relationships within *A. amphibius sensu lato* had caused a long-standing debate. The phylogenetic relationships among *Arvicola* were reconstructed using the mitochondrial cytochrome *b* gene. Four lineages within *A. amphibius s. l.* were identified with good support: Western European, Eurasiatic, Italian, and Turkish lineages. Fossorial and aquatic forms were found together in all well-sampled lineages, evidencing that ecotypes do not correspond to distinct species. However, the Western European lineage mostly includes fossorial forms whereas the Eurasiatic lineage tend to include mostly aquatic forms. A morphometric analysis of skull shape evidenced a convergence of aquatic forms of the Eurasiatic lineage towards the typically aquatic shape of *A. sapidus*. The fossorial form of the Western European lineage, in contrast, displayed morphological adaptation to tooth-digging behavior, with expanded zygomatic arches and proodont incisors. Fossorial Eurasiatic forms displayed intermediate morphologies. This suggest a plastic component of skull shape variation, combined with a genetic component selected by the dominant ecology in each lineage. Integrating genetic distances and other biological data suggest that the Italian lineage may correspond to an incipient species (*A. italicus*). The three other lineages most probably correspond to phylogeographic variations of a single species (*A. amphibius*), encompassing the former *A. amphibius*, *A. terrestris*, *A. scherman* and *A. monticola*.

Introduction

The extension of phylogeographical studies has led to the increasing recognition that many species traditionally identified based on morphological traits encompass several genetic distinct forms that constitute "cryptic species" [e.g. (Bryja et al., 2014; Mouton et al., 2017)]. Slow morphological divergence, as a probable consequence of stabilizing selection, may be responsible for the limited phenotypic signature of these cryptic species. Yet, morphology, inclusive osteological traits, varies according to ecological conditions, including diet (Michaux, Chevret, & Renaud, 2007) but also way-of-life such as digging behavior, which exerts strong functional demands on the skull (Gomes Rodrigues, Šumbera, & Hautier, 2016). As a consequence, ecological versatility may lead to morphological convergence blurring the signature of genetic divergence between species. Assessing the evolutionary units involved in such cases is crucial to understand the selective context driving the genetic and morphological divergence.

Water voles of the genus *Arvicola* constitute an emblematic example of the controversies that may arise regarding ecological forms. Fossorial and semi-aquatic forms have been described as species (*A. terrestris*, Linnaeus, 1758, type locality Uppsala, Sweden and *A. amphibius*, Linnaeus, 1758, type locality England) already by Linnaeus in 1758. Later on, up to seven species have been described (Miller et al., 2012). By combining chromosomal and ecological data, only three species were thereafter proposed (Heim de Balsac & Guislain, 1955): the Southern water vole *A. sapidus*, Miller, 1908, with 2n = 40, *A. terrestris* for semi-aquatic forms with 2n = 36, and *A. scherman*, Shaw, 1801, for fossorial forms with 2n = 36.

The status of *A. sapidus* was subject to little debate but controversy persisted regarding the aquatic and fossorial forms *A. terrestris*/*A. scherman*: considered as a single polytypic species (Wilson & Reeder, 1993), or valid distinct species: *A. amphibius* and *A. scherman* (Wilson & Reeder, 2005). More recently, the Italian water vole was proposed as a separate species (*A. italicus*, Savi, 1839) (Castiglia et al., 2016), while the aquatic and fossorial forms remained considered as separate species with distinct geographic distribution, under the names of *A. amphibius* and *A. monticola*, de Sélys Longchamps, 1838 (Pardiñas et al., 2017). Even more recently, Mahmoudi, Maul, Khoshyar, & Darvish (2019) identified in Iran another species, *A. persicus*. Hence, the genus *Arvicola* currently includes five species: *amphibius, italicus, monticola, sapidus* and *persicus* (Mahmoudi et al., 2019; Pardiñas et al., 2017).

Yet, an increasing genetic sampling brought new fuel in the debate, showing that the ecological forms were not systematically associated with distinct clades. Fossorial and aquatic

forms have been found to coexist in the Italian water vole (Castiglia et al., 2016) and in *A. scherman* (Kryštufek et al., 2015). The limited sampling of *A. monticola* precluded to reliably asses the variation in this presumed fossorial clade (Mahmoudi et al., 2019).

The present study therefore aims at a clarification of the phylogenetic pattern within European water voles, by compiling published and new cytochrome b sequences, with the aim to improve the geographic coverage and representation of the two ecological forms. This genetic approach was complemented by a morphometric analysis of skull shape variations of aquatic and fossorial forms, in order to assess the patterns of morphological differentiation and possible convergences.

Material and Methods

The terminology used thereafter is the following. The Southern water vole, *A. sapidus,* and the Iranian water vole, *A. persicus,* were named by their Latin name. The other water voles were designed as "water voles" or *Arvicola amphibius* considered *sensu lato,* hence including both fossorial and aquatic water voles (including specimens labelled as *amphibius, monticola, scherman* and *terrestris*). The status of the Italian water vole will be discussed, but the name "*italicus*" was tentatively retained.

Material for genetics

The genetic sampling original to this study included 143 tissue samples of *Arvicola amphibius s. l.* from Belgium, Denmark, France, Germany, Great Britain and Spain, two specimens identified as *A. scherman* from Spain, as well as two samples of *Arvicola sapidus* (Table S1). Most of the samples were attributed to fossorial or aquatic forms, based on field evidences: fossorial forms were trapped in tumuli. It was completed with sequences available in GenBank for *A. amphibius* (89), *A. scherman* (2), *A. sapidus* (12) and *A. persicus* (14) (Table S1). The complete dataset for *A. amphibius s. l.* comprised 236 sequences from 102 localities (Table S1, Figure 1A).

Material for morphometrics

The material available for morphometric studies (Table S2) corresponded to 223 skulls. It included various fossorial populations from France and Western Switzerland. The Eurasiatic lineage (sensu (Castiglia et al., 2016)) was sampled by aquatic populations from Finland, Denmark, and Belgium. Water voles from Ticino in Southern Switzerland were labelled as

italicus and represented the Italian lineage (Brace et al., 2016; Castiglia et al., 2016). Specimens from various localities in France and Spain represented the sister species *A. sapidus*.

In three populations (Chapelle d'Huin, La Grave, and Prangins), sex information was available and allowed to test for sexual dimorphism. Almost all specimens corresponded to adult and sub-adult specimens. The specimens are stored in the collections of the Centre de Biologie et Gestion des Populations (Baillarguet, Montferrier-sur-Lez, France), the Muséum d'Histoire Naturelle (Geneva, Switzerland) and the Université de Liège (Belgium).

Genetic analysis

DNA was extracted from ethanol-preserved tissue of *Arvicola*, using the DNeasy Blood and Tissue kit (Qiagen, France) following the manufacturer instructions. The cytochrome *b* gene sequence was amplified using previously described primers L7 (5-ACCAATGACATGAAAAATCATCGTT-3) and H6 (5'-TCTCCATTTCTGGTTTACAAGAC-3') (Montgelard, Bentz, Tirard, Verneau, & Catzeflis, 2002). PCRs were carried out in 50 µl volume containing 12.5 µl of each 2 mM primers, 1 µl of 10 mM dNTP, 10 µl of reaction buffer (Promega), 0.2 µl of 5 U/µl Promega *Taq* DNA polymerase and approximately 30 ng of DNA extract. Amplifications were performed using one activation step (94°C/4 min) followed by 40 cycles (94°C/30 s, 50°C/60 s, 72°C/90 s) with a final extension step at 72°C for 10 min. PCR products (1243 bp long) were send to Macrogen (Seoul, Korea) for sequencing.

The sequences generated were visualized and analyzed using Seqscape (Applied Biosystems) or CLC Workbench (Qiagen) and aligned with Seaview v4 (Gouy, Guindon, Gascuel, & Lyon, 2010). All the new sequences were submitted to GenBank: accession number LR746349 to LR746495. The final alignment comprised 264 sequences of *Arvicola*, 147 new ones and 117 retrieved from GenBank. Sequences of *Microtus arvalis, Myodes glareolus, Eothenomys melanogaster,* and *Ellobius tancrei* were used as outgroups. This resulted in a final alignment comprising 268 sequences and 911 positions (Alignment S1) after the removal of the sites with more than 10% of missing data. The best model fitting our data (GTR+I+G) was selected with jModelTest (Darriba, Taboada, Doallo, & Posada, 2012) using the Akaike criterion (Akaike, 1973). The phylogenetic tree was reconstructed using maximum likelihood with PhyMl 3.0 (Guindon et al., 2010) and Bayesian inference with MrBayes v3.2 (Ronquist et al., 2012). Robustness of the nodes were estimated with 1000 boostrap replicates with PhyMl and posterior probability with MrBayes. Markov chain Monte Carlo (MCMC)

analyses were run independently for 20 000 000 generations with one tree sampled every 500 generations. The burn-in was graphically determined with Tracer v1.6 (A. Rambaut, Suchard, Xie, & Drummond, 2014). We also checked that the effective sample sizes (ESSs) were above 200 and that the average standard deviation of split frequencies remained <0.05 after the burn-in threshold. We discarded 10% of the trees and visualized the resulting tree with Figtree v1.4 (Rambaut, 2012). MEGA 7 (Kumar, Stecher, & Tamura, 2016) was used to estimate K2P distance between and within lineages. We use POPART (Leigh & Bryant, 2015) to reconstruct a median joining network of haplotypes (Bandelt, Forster, & Rohl, 1999). This analysis was restricted to the 236 sequences of *A. amphibius*, and the corresponding haplotypes were determined with DnaSP v6 (Rozas et al., 2017).

Morphometric analyses

Each skull was photographed in ventral and lateral views using a Canon EOS 400D digital camera. The ventral view was described by a configuration of 22 landmarks and 13 sliding semi-landmarks along the zygomatic arch. The lateral view was described using a configuration of 24 landmarks and 39 sliding semi-landmarks (Figure S1). All landmarks and sliding semi-landmarks were digitized using TPSdig2 (Rohlf, 2010). The sampling included 189 skulls in ventral view and 186 ones in lateral view (Table S2).

The configurations of landmarks and semi-landmarks were superimposed using a generalized Procrustes analysis (GPA) standardizing size, position and orientation while retaining the geometric relationships between specimens (Rohlf & Slice, 1990). During the superimposition, semi-landmarks were allowed sliding along their tangent vectors until their positions minimize the shape between specimens, the criterion being here bending energy (Bookstein, 1997). A Principal Component Analysis (PCA) was performed on the resulting aligned coordinates. Relationships between difference groups were investigated using a Canonical Variate Analysis (CVA) which aims at separating groups by looking for linear combinations of variables that maximize the between-group to within-group variance ratio. By standardizing within-group variance, this method may be efficient for evidencing phylogenetic relationships (Renaud, Dufour, Hardouin, Ledevin, & Auffray, 2015). In order to reduce the dimensionality of the data, the CVA was performed on the set of Principal Components (PC) totaling more than 95% of the variance.

Skull size was estimated using the centroid size (square root of the sum of the squared distances from each landmark to the centroid of the configuration). Size differences were tested using analyses of variance (ANOVA).

Geometric differences between groups and regression models were investigated using procedures adapted for Procrustes data (Procrustes ANOVA). Using this approach, the Procrustes distances among specimens are used to quantify explained and unexplained components of shape variation, which are statistically evaluated via permutation (here, 9999 permutations) (Adams et Otárola-Castillo 2013). Allometric variations were investigated, investigating skull shape as a function of skull size. The effect of a grouping variable combining genetic and ecological information ("GxE") was also included (Table S2), allowing to test if the allometric slopes were different between the groups. Visualization were obtained using the Common Allometric Component (CAC) derived from this allometry analysis (Adams et al. 2013). Procrustes superimposition, PCA and Procrustes ANOVA were performed using the R package geomorph (Adams & Otárola-Castillo, 2013). The CVA was computed using the package Morpho (Schlager, 2017).

Results

Genetics

On the phylogenetic tree (Figure 2, see Figure S2 for the complete phylogeny) the three groups corresponding to *A. sapidus*, *persicus* and *amphibius s. l.* were well supported (PP≥0.93, BP≥82) with *A. amphibius* more closely related to *A. persicus* (PP=0,93, PP=72) than to *A. sapidus*. The phylogenetic tree as well as the network (Figure 1B) evidenced four lineages within *A. amphibius s. l.*. Most of the sequences of *amphibius s. l.* belonged to two lineages: Lineage 1 (L1) and Lineage 2 (L2). L1 was present in France, Spain, Switzerland and the North of Great Britain and comprises mostly fossorial forms. This lineage was divided into two sub-groups: the first one with samples from France and Spain and the second one with samples from Great Britain, Switzerland and France. The two specimens identified as *A. scherman* belonged to this lineage. L2 had a large repartition area from the south of Great Britain to Russia (East), Finland (North) and Romania (South) and it comprised more aquatic than fossorial forms. The two remaining lineages were restricted to Turkey, Lineage 3 (L3) with aquatic forms only and Italy, Lineage 4 (L4) with both aquatic and fossorial forms (Figure 2, Figure S2 and Figure 1C). In several French localities (Chapelle d'Huin, Doubs; Val d'Ajol, Vosges; Vauconcourt, Haute-Saône; Vigeois, Corrèze), a co-occurrence of lineages 1 and 2 was documented. In all cases, L1 was dominant and the population mostly fossorial.

Regarding the amount of genetic divergence, *A. sapidus*, *A. persicus* and *A. amphibius s. l.*

appeared well differentiated (K2P distances ≥ 7.2). L3 was closely related to L2 (K2P = 2.9) whereas L4, which correspond to *A. italicus*, was the most divergent (4.4 < K2P < 5.1) within *A. amphibius s. l.* (Table 1).

Morphometrics

Sexual dimorphism. – Sexes displayed very similar skull size and shape. No difference was detected for the size of the skull in ventral view (ANOVA on Ventral Centroid Size: Chapelle d'Huin P = 0.3031; La Grave P = 0.8706; Prangins P = 0.9799) and in lateral view (ANOVA on Lateral Centroid Size: Chapelle d'Huin P = 0.1358; La Grave P = 0.3575; Prangins P = 0.9576). Similarly, skull shape was not different between sexes, for the skull in ventral view (Procrustes ANOVA on ventral skull shape: Chapelle d'Huin P = 0.6130; La Grave P = 0.4556; Prangins P = 0.8309) as for the skull in lateral view (Procrustes ANOVA on lateral skull shape: Chapelle d'Huin P = 0.1918; La Grave P = 0.4337; Prangins P = 0.7164). All animals were therefore pooled in subsequent analyses.

Skull size. – The different groups of water voles significantly differed in skull size (ANOVA on CSventral and CSlateral: P < 0.0001). Skulls of water voles, being fossorial or aquatic, were smaller than those of *A. sapidus* (Figure 3). Important size variation occurred within *A. amphibius s.l.*. The aquatic populations of L2 were especially variable in size, the Belgian one being almost as large as *A. sapidus* whereas skulls from Finnish *A. amphibius* were among the smallest. Important size variation also occurred within populations belonging to L1.

Skull shape in ventral view. – The variation of skull shape in ventral view was structured in two groups on the first two axes of a PCA on the aligned coordinates (Figure 4A). These two groups opposed aquatic forms (*A. sapidus* and specimens belonging to L4 and L2) to fossorial forms belonging to L1. The L2 fossorial population from Alsace plotted between these two main groups, whereas the Slovakian specimens, presumably also belonging to L2 given the geographic extension of this lineage, plotted within the range of variation of fossorial L1. The fossorial specimens from Western Switzerland (Arzier and Prangins), presumably belonging to L1, and the population from Chappelle d'Huin, characterized by a genetic mixing of L1 and L2, shared the same range of variation as fossorial L1. The shape change from negative to positive PC1 scores, and hence from aquatic to fossorial forms, mostly involved a lateral extension of the zygomatic arch and a forward displacement of the incisor tip.

Both fossorial and aquatic groups displayed an important variation along PC1 and PC2. This was related to an important allometry (Figure 4B) (Procrustres ANOVA on aligned coordinates: shape ~CS: P < 0.001). A Procrustes ANOVA including as factors centroid size

and the GxE grouping indicated a significant influence of both factors ($P < 0.001$) but supported the hypothesis of parallel slopes. These parallel trends in the different groups were visualized along the CAC (Figure 4B), which involved discrete shape changes with a slight backward shift of the incisor tip, and a compression of the posterior part of zygomatic arch (Figure 4C). For similar CAC scores, aquatic forms tended to display larger skulls, especially those of *A. sapidus*.

The PCA on the aligned coordinates was further used to reduce the dimensionality of the data. The first 23 axes totaled 95% of the total variance and were used in a CVA, the grouping factors being the geographical groups (Figure 4D). As the PCA, the CVA tended to separate aquatic and fossorial forms; but it more clearly isolated *A. sapidus* and to a lesser extent the population from Ticino corresponding to the genetically well-differentiated L4. Despite their ecological heterogeneity, populations affiliated to L2, including the fossorial population from Alsace and the Slovakian population of unknown ecology, tended to share negative CVA1 scores. All other fossorial populations, affiliated to L1 or with a mixing of L1 and L2, plotted towards positive CVA1 scores.

The morphological differences between some groups means were further visualized (Figure 4C). The change from the aquatic *A. sapidus* and to the typical fossorial water voles from the L1 mostly involved a lateral expansion of the zygomatic arch, a posteriorly compressed brain case and a forward shift of the incisor tip. The lateral expansion of the zygomatic arch is also observed in the shape change from aquatic to fossorial ecology within L2. This change within L2 is however of a lesser magnitude than the change between the well differentiated units *A. sapidus* and fossorial L1.

Skull shape in lateral view. – The PCA on the aligned coordinates of the skull in lateral view (Figure 5A) provided a less clear structure than the one of the skull in ventral view. Aquatic and fossorial forms tended to segregate along PC1, but with a considerable overlap. The shape changes along this axis involved a proodont shift of the incisor, a ventral expansion of the zygomatic arch, and a curvature of the brain case, but these shape changes corresponded both to a difference between aquatic and fossorial forms, and to an extensive variation within each ecological form.

This extensive variation is largely due to allometry (Procrustes ANOVA: shape ~ CS: $P < 0.001$). As for the ventral view, the different groups had parallel allometric slopes which were shifted between groups (Figure B; shape ~CS: $P < 0.001$, ~GxE: $P < 0.001$). The common allometric trend corresponded to a flattening of the brain case and a slight backward shift of the incisor tip (Figure 5C).

The first 29 axes of the PCA totaled 95% of variance and were used in a CVA (Figure 5D). *A. sapidus* and the Ticino population from L4 appeared as well divergent along the first CVA axis, explaining most of the variation. All other populations were close to each other. Whatever their ecology, populations attributed to L2, including that from Slovakia, were tightly clustered towards CVA1 scores close to zero. All fossorial populations belonging to L1, or where lineages 1 and 2 co-occur, were clustered towards negative CVA1 scores. The shape change between aquatic and fossorial group means (Figure 5C) allowed to better assess the shape changes related to ecology. The difference between *A. sapidus* and the fossorial L1 clearly showed the proodont shift of the incisor. This shift is also characteristic, although at a lesser magnitude, in the transition from aquatic to fossorial forms within L2; this was associated with a downward shift of the zygomatic arch.

Discussion

Phylogeny evidenced widespread ecological versatility

The molecular data confirmed the separation of *A. sapidus* and *A. persicus* and other water voles as in Mahmoudi et al. (2019). They further evidenced four lineages within the "European water vole" *A. amphibius s. l*: (1) L1, with a Western European distribution (Castiglia et al., 2016) and a dominance of fossorial forms. This lineage was found mostly in France, the neighboring Western Switzerland, and in Northern areas of Great Britain. (2) A widespread Euroasiatic L2 (Castiglia et al., 2016; Kryštufek et al., 2015), present from Belgium and Germany to the West up to Eastern parts of Russia. This lineage showed a dominance of aquatic forms. Note that the co-occurrence of lineages 1 and 2 in Great Britain has been shown to be the consequence of a colonization in two waves, the second partly replacing the first *ca* 12-8 kyr BP (Brace et al., 2016; Searle et al., 2009). (3) Related to the Eurasiatic L2, a third lineage (L3) was found, up to now, in Turkey (Kryštufek et al., 2015). (4) L4, characteristic of Italy and the neighboring Southern Switzerland (Ticino) (Brace et al., 2016; Castiglia et al., 2016). It was the most divergent of the lineages *within A. amphibius s. l.* and corresponded to the proposed species *A. italicus*.

Confirming recent results (Castiglia et al., 2016; Kryštufek et al., 2015), the present study undermined the interpretation of fossorial and aquatic forms as distinct genetic units. Instead, ecological versatility was evidenced within at least three out of four lineages, aquatic and fossorial forms being mixed in the lineages 1 (Western Europe), 2 (Euroasiatic) and 4 (Italian). The reduced sampling of L3 (Turkey) precluded any conclusions regarding this

lineage. Clearly, aquatic and fossorial forms do not constitute separate species in water voles *A. amphibius s. l.* (Kryštufek et al., 2015).

The genetic distances separating the lineages typically fell within a "grey zone", where values typical for intraspecific divergence and those associated with interspecific divergence overlap (~3 < K2P < ~6) (Barbosa, Pauperio, Searle, & Alves, 2013). With K2P values between 4 and 5, they typically corresponded to the range of differentiation between phylogenetic lineages within rodent species (Michaux, Magnanou, Paradis, Nieberding, & Libois, 2003; Paupério et al., 2012), and slightly below values corresponding to the differentiation between species (Amori, Gippoliti, & Castiglia, 2009; Kohli et al., 2014; Vallejo & González-Cózatl, 2012).

A two-fold morphological signature

The morphological differentiation among water voles was assessed using two widely used methods in morphometrics: PCA and CVA. These methods provided different structures between populations in the corresponding morphospaces, the PCA emphasizing the morphological differences related to ecology, opposing aquatic and fossorial voles whatever their phylogenetic background, while the CVA retrieved a signal more related to the phylogenetic structure. This discrepancy is related to the properties of the methods. The PCA decomposes the total variance, and therefore is highly impacted by extensive within-group variation related to ontogenetic and ecological changes. In contrast, by expressing between-group differences while standardizing within-group variance, the CVA can put forward more discrete traits characterizing different lineages. It is confirmed here as an efficient tool for showing phylogenetic relationships (Renaud et al., 2015).

Ecological forms and their adaptive morphological signature on skull shape

The chisel-tooth digging behavior is known to exert strong physical loads on the skull, and thus to constitute a strong selective pressure leading to morphological convergence in skull shape across different rodent families (Gomes Rodrigues et al., 2016; Samuels & Van Valkenburgh, 2009). Accordingly, an important skull shape differentiation opposed aquatic to fossorial groups. Chisel-tooth digging especially requires powerful masseter muscles to move the mandible into occlusion. This muscle originates along the zygomatic arch and inserts on the angular process of the mandible. As a consequence, the expanded zygomatic arch is typical for fossorial rodents (Samuels & Van Valkenburgh, 2009). Proodont incisors are also a typical trait for fossorial rodents, favoring the process of biting in the substrate (Samuels & Van Valkenburgh, 2009). The signal found in *Arvicola* skulls agrees with these general

ecomorphological characteristics: fossorial populations display an expanded angular processes on the mandible (Durão, Ventura, & Muñoz-Muñoz, 2019), especially visible in ventral view, and proodont incisors, a trait that is best traced in lateral view. Altogether, the morphometric differentiation between fossorial and aquatic water voles documents an integrated adaptive response to the functional demand of tooth digging.

Opposite to fossorial water voles, the skulls of *A. sapidus* display extreme skull shapes, without overlap with other water vole populations, even aquatic ones. This pronounced morphological differentiation [(Durão et al., 2019); this study] is likely the combined result of a genetic divergence supportive of a valid species, and of the absence of ecological versatility in this taxon, always displaying a semi-aquatic way of life.

Within *A. amphibius s.l.*, fossorial and aquatic populations tended to be well differentiated. This was especially true for the fossorial populations of the Western European L1 (dominantly fossorial) and the aquatic populations of the Euroasiatic L2 (mostly aquatic). The Alsacian fossorial population of L2 was shifted towards the fossorial populations of L1, but still displayed an intermediate morphology between aquatic and fossorial forms. This suggests that the genetic divergence between the two lineages was enough to accumulate adaptations to the dominant ecology. However, the persistent ecological versatility triggers local adaptation in case of a switch to the alternative strategy. This response in skull shape probably include a plastic component, since bone permanently remodel in response to mechanical stress produced by muscular activity, including in the context of digging activity (Durão et al., 2019; Ventura & Casado-Cruz, 2011) .

Regarding size, fossorial forms of *A. amphibius s.l* were mentioned to be smaller than the aquatic forms in the Euroasiatic region (Kryštufek et al., 2015) but the reverse in Italy (Castiglia et al., 2016). The present study did not evidence any clear trend between lineages or forms, to the exceptions of the clearly larger *A. sapidus*. The hypothesis that burrowing would favor small-sized animals, because of reduced digging costs (Durão et al., 2019) is therefore not supported within *A. amphibius s. l.*, although local ecological conditions may be involved in the important geographic differences in skull size even within the same lineage. The age structure of the sampled populations may explain at least partly differences in the size distribution, depending whether or not young animals were dominant at the time of trapping (Renaud, Hardouin, Quéré, & Chevret, 2017). Whatever its cause, size variation was associated to allometric variation of skull shape. *A. sapidus*, and fossorial and aquatic forms of *A. amphibius s.l.* shared parallel allometric trajectories, fossorial forms showing more "adult-like" morphologies than aquatic ones for a given size. In that respect, the evolution of

fossorial forms may be seen as heterochronic (Cubo, Ventura, & Casinos, 2006). However, the morphological signal directly related to allometry was of limited amount and did not match the differences related to ecology. Adaptive and plastic response to the functional demand of chisel-tooth digging thus appears a more likely explanation of the morphological differences between groups. The corresponding morphological characteristics seem to appear early in life, with a conservation of the ontogenetic trajectory in aquatic and fossorial water voles.

Fossorial vs. aquatic: an oversimplified classification

The Italian lineage (L4) was represented in the morphometric study by a sole population from Ticino in Switzerland. This population was within the range of aquatic populations in PCA morphospaces, in agreement with its dominant ecology. In the CVA morphospaces, it clearly departed from the other lineages of *A. amphibius s. l.*, suggesting a morphological signature of the Italian lineage.

Similarly, populations belonging to L2 appeared clustered in the CVA plots, especially in lateral view, suggesting a morphological signature for this lineage as well. However, in the PCA morphospaces, these populations ranged from a typically aquatic to a fossorial morphology (considering the Slovakian population as likely belonging to this lineage), with the Alsacian population being intermediate in shape. This illustrates the ecological versatility of water voles when facing environmental changes. Furthermore, if some forms are attached all year to water, and some inhabit dry areas, some animals switch between both habitats during the year (Wust-Saucy, 1998). In front of this ecological versatility even on very short time scales, the expectation of discrete fossorial and aquatic morphotypes may be inadequate (Kryštufek et al., 2015). Typical aquatic voles from the dominantly aquatic L2 and typical fossorial voles from L1 might represent endmembers of a phenotypic continuum, the skull morphology being dependent both on the genetic background and the ecological conditions of growth.

Taxonomic implications

The strength of the present study relies on the extensive sampling of water voles across Europe. However, the taxonomic conclusions are only based on a mitochondrial gene (cytochrome *b*) and the pattern of morphological divergence of the skull. Nuclear data would be required to validate these conclusions, but the only data available so far, based on the Interphotoreceptor Retinoid Binding Protein **(**IRBP) gene, remained inconclusive for *Arvicola*

amphibius s.l. (Mahmoudi et al., 2019).

In agreement with previous studies, genetic and morphometric results support the specific status for the Southern water-vole *A. sapidus* Miller, 1908 (type locality Santo Domingo de Silos, Burgos Province, Spain). Its genetic divergence from the other lineages (K2P > 7) was close to what is observed between other valid rodent species (Amori et al., 2009; Barbosa et al., 2013). The genetic divergence was also very high for the species described in Iran: *A. persicus* (K2P > 9) (Mahmoudi et al., 2019). Nuclear and mitochondrial data support the specific status of these two species (Mahmoudi et al., 2019).

The Italian lineage is the most differentiated within *A. amphibius s.l.* (K2P ≥4.4). Reproductive isolation has been evidenced between animals from the north and south sides of the Swiss Alps, populations that can be nowadays attributed to the Western European L1 and the Italian L4 [(Morel, 1979) in (Castiglia et al., 2016)]. This supports the Italian lineage as an incipient species: *A. italicus* (type locality Pisa, Italy).

The other lineages (Western European L1, Euroasiatic L2, and Turkish L3) correspond partially to entities that have been even recently proposed as separate species: *A. amphibius* and *A. monticola* (Mahmoudi et al., 2019). In Mahmoudi et al. (2019), *A. monticola* was proposed for fossorial voles from Western Europe (Switzerland and Spain), which are included in our Lineage 1, whereas *A. amphibius* include Siberian (aquatic) and European (aquatic and fossorial) voles, which are included in our Lineage 2. The genetic divergence between lineages 1, 2 and 3 was rather low (K2P = 2.9-4.1), hence they are most likely phylogenetic lineages related to repeated isolations in glacial refugia during the Quaternary climatic fluctuations (Michaux, Chevret, Filippucci, & Macholan, 2002; Taberlet, Fumagalli, Wust-Saucy, & Cosson, 1998). Furthermore, our extensive sampling evidenced that the two main lineages (1 and 2) can co-occur in the same localities at the fringe of their respective distribution area. In the population of Chapelle d'Huin, (Doubs, France), showing a co-occurrence of lineages 1 and 2, specimens display a skull shape typical of L1. This suggests that exchanges between the two lineages occur at the nuclear level. The three lineages, which present low genetic divergence, should thus be attributed to a single species: *A. amphibius* (Linné, 1758) (including the former recognized species *amphibius, monticola, sherman* and *terrestris)*.

Acknowledgements

The authors are deeply indebted to all contributors who provided samples from the different regions, or helped in the preparation of the material: E. Aarnink, H. Ansorge, T. Asferg, K. Baumann, S. Blome, T. Büchner, P. Callesen, J. Caspar, F. Catzeflis, F. Chanudet, J.-F. Cosson, G. Couval, C. Crespe, M. Debussche, the Derek Gow Consultancy Ltd, S. Drewes, H. Dybdahl, A. Globig, J.-D. Graf, B. Hammerschmidt, A. Hellemann, H. Henttonen, J. Huitu, J. Jacob, D. Kaufmann, N. Kratzmann, C. Kretzschmar, V. Kristensen, E. Krogh Pedersen, J. Lang, P. Lestrade, D. Maaz, C. Maresch, C. Martins, A. Meylan, J.Morel, E. Perreau, K. Plifke, B. Pradier, F. Raoul, D. Reil, S. Reinholdt, U. M. Rosenfeld, M. Ruedi, T. Ruys, M. Schlegel, S. Schmidt, T. Schröder, J. Schröter, H. Sheikh Ali, N. Stieger, J. Struyck, J. Thiel, F. Thomas, D. Truchetet, J.R. Vericad, G. Villadsen, K. Wanka, U. Wessels, A. Wiehe, D. Windolph, R. Wolf, T. Wollny, I. Yderlisere. M.-P. Bournonville is particularly thanked for her participation to the acquisition of the genetic data.

This work was performed using the computing facilities of the CC LBBE/PRABI. Johan Michaux benefited from FRS-FNRS grants (“directeur de recherches”). The sequencing of the cytochrome *b* gene was performed using private funding from the Conservation Genetics Laboratory of the University of Liège.

References

Adams, D. C., & Otárola-Castillo, E. (2013). geomorph: an r package for the collection and analysis of geometric morphometric shape data. *Methods in Ecology and Evolution*, *4*(4), 393–399. https://doi.org/10.1111/2041-210X.12035

Akaike, H. (1973). Information theory as an extension of the maximum likelihood principle. In B. N. Petrov & F. Csaki (Eds.), *Second International Symposium on Information Theory* (pp. 267–281). https://doi.org/10.2307/2334537

Amori, G., Gippoliti, S., & Castiglia, R. (2009). European non-volant mammal diversity: Conservation priorities inferred from phylogeographic studies. *Folia Zoologica*, *58*(3), 270–278.

Bandelt, H. J., Forster, P., & Rohl, A. (1999). Median-joining networks for inferring intraspecific phylogenies. *Molecular Biology and Evolution*, *16*(1), 37–48. https://doi.org/10.1093/oxfordjournals.molbev.a026036

Barbosa, S., Pauperio, J., Searle, J. B., & Alves, P. C. (2013). Genetic identification of Iberian

494 rodent species using both mitochondrial and nuclear loci: application to noninvasive
495 sampling. *Molecular Ecology Resources*, *13*(1), 43–56. https://doi.org/10.1111/1755-
496 0998.12024
497 Bookstein, F. L. (1997). Landmark methods for forms without landmarks: morphometrics of
498 group differences in outline shape. *Medical Image Analysis*, *1*(3), 225–243.
499 https://doi.org/10.1016/S1361-8415(97)85012-8
500 Brace, S., Ruddy, M., Miller, R., Schreve, D. C., Stewart, J. R., & Barnes, I. (2016). The
501 colonization history of British water vole (Arvicola amphibius (Linnaeus, 1758)):
502 Origins and development of the Celtic fringe. *Proceedings of the Royal Society B:*
503 *Biological Sciences*, *283*(1829). https://doi.org/10.1098/rspb.2016.0130
504 Bryja, J., Radim, Š., Meheretu, Y., Aghová, T., Lavrenchenko, L. A., Mazoch, V., …
505 Verheyen, E. (2014). Pan-African phylogeny of Mus (subgenus Nannomys) reveals one
506 of the most successful mammal radiations in Africa. *BMC Evolutionary Biology*, *14*(1),
507 256. https://doi.org/10.1186/s12862-014-0256-2
508 Castiglia, R., Aloise, G., Amori, G., Annesi, F., Bertolino, S., Capizzi, D., … Colangelo, P.
509 (2016). The Italian peninsula hosts a divergent mtDNA lineage of the water vole,
510 Arvicola amphibius s.l., including fossorial and aquatic ecotypes. *Hystrix*, *27*(2).
511 https://doi.org/10.4404/hystrix-27.2-11588
512 Cubo, J., Ventura, J., & Casinos, A. (2006). A heterochronic interpretation of the origin of
513 digging adaptations in the northern water vole, Arvicola terrestris (Rodentia:
514 Arvicolidae). *Biological Journal of the Linnean Society*, *87*(3), 381–391.
515 https://doi.org/10.1111/j.1095-8312.2006.00575.x
516 Darriba, D., Taboada, G. L., Doallo, R., & Posada, D. (2012). jModelTest 2: more models,
517 new heuristics and parallel computing. *Nature Methods*, *9*(8), 772–772.
518 https://doi.org/10.1038/nmeth.2109
519 Durão, A. F., Ventura, J., & Muñoz-Muñoz, F. (2019). Comparative post-weaning ontogeny
520 of the mandible in fossorial and semi-aquatic water voles. *Mammalian Biology*, *97*, 95–
521 103. https://doi.org/10.1016/j.mambio.2019.05.004
522 Gomes Rodrigues, H., Šumbera, R., & Hautier, L. (2016). Life in Burrows Channelled the
523 Morphological Evolution of the Skull in Rodents: the Case of African Mole-Rats
524 (Bathyergidae, Rodentia). *Journal of Mammalian Evolution*, *23*(2), 175–189.
525 https://doi.org/10.1007/s10914-015-9305-x
526 Gouy, M., Guindon, S., Gascuel, O., & Lyon, D. (2010). SeaView version 4: A multiplatform
527 graphical user interface for sequence alignment and phylogenetic tree building.

Molecular Biology and Evolution, *27*(2), 221–224. https://doi.org/10.1093/molbev/msp259

Guindon, S., Dufayard, J.-F., Lefort, V., Anisimova, M., Hordijk, W., & Gascuel, O. (2010). New algorithms and methods to estimate maximum-likelihood phylogenies: assessing the performance of PhyML 3.0. *Systematic Biology*, *59*(3), 307–321. https://doi.org/10.1093/sysbio/syq010

Heim de Balsac, H., & Guislain, R. (1955). Évolution et spéciation des campagnols du genre Arvicola en territoire français. *Mammalia*, *19*(3), 367–390. https://doi.org/10.1515/mamm.1955.19.3.367

Kohli, B. A., Speer, K. A., Kilpatrick, C. W., Batsaikhan, N., Damdinbaza, D., & Cook, J. A. (2014). Multilocus systematics and non-punctuated evolution of Holarctic Myodini (Rodentia: Arvicolinae). *Molecular Phylogenetics and Evolution*, *76*, 18–29. https://doi.org/10.1016/j.ympev.2014.02.019

Kryštufek, B., Koren, T., Engelberger, S., Horváth, G. F., Purger, J. J., Arslan, A., … Murariu, D. (2015). Fossorial morphotype does not make a species in water voles. *Mammalia*, *79*(3), 293–303. https://doi.org/10.1515/mammalia-2014-0059

Kumar, S., Stecher, G., & Tamura, K. (2016). MEGA7: Molecular Evolutionary Genetics Analysis Version 7.0 for Bigger Datasets. *Molecular Biology and Evolution*, *33*(7), 1870–1874. https://doi.org/10.1093/molbev/msw054

Leigh, J. W., & Bryant, D. (2015). POPART: full-feature software for haplotype network construction. *Methods in Ecology and Evolution*, *6*(9), 1110–1116. https://doi.org/10.1111/2041-210X.12410

Mahmoudi, A., Maul, L. C., Khoshyar, M., & Darvish, J. (2019). Evolutionary history of water voles revisited: confronting a new phylogenetic model from molecular data with the fossil record. *Mammalia*. https://doi.org/10.1515/mammalia-2018-0178

Michaux, J., Chevret, P., & Renaud, S. (2007). Morphological diversity of Old World rats and mice (Rodentia, Muridae) mandible in relation with phylogeny and adaptation. *Journal of Zoological Systematics and Evolutionary Research*, *45*(3), 263–279. https://doi.org/10.1111/j.1439-0469.2006.00390.x

Michaux, J. R., Chevret, P., Filippucci, M.-G., & Macholan, M. (2002). Phylogeny of the genus Apodemus with a special emphasis on the subgenus Sylvaemus using the nuclear IRBP gene and two mitochondrial markers: cytochrome b and 12S rRNA. *Molecular Phylogenetics and Evolution*, *23*(2), 123–136. https://doi.org/10.1016/S1055-7903(02)00007-6

562 Michaux, J. R., Magnanou, E., Paradis, E., Nieberding, C., & Libois, R. (2003).
563 Mitochondrial phylogeography of the Woodmouse (Apodemus sylvaticus) in the
564 Western Palearctic region. *Molecular Ecology*, *12*(3), 685–697.
565 Miller, W., Schuster, S. C., Welch, A. J., Ratan, A., Bedoya-Reina, O. C., Zhao, F., …
566 Lindqvist, C. (2012). Polar and brown bear genomes reveal ancient admixture and
567 demographic footprints of past climate change. *Proceedings of the National Academy of*
568 *Sciences*, *109*(36), E2382–E2390. https://doi.org/10.1073/pnas.1210506109
569 Montgelard, C., Bentz, S., Tirard, C., Verneau, O., & Catzeflis, F. M. (2002). Molecular
570 systematics of sciurognathi (rodentia): the mitochondrial cytochrome b and 12S rRNA
571 genes support the Anomaluroidea (Pedetidae and Anomaluridae). *Molecular*
572 *Phylogenetics and Evolution*, *22*(2), 220–233. https://doi.org/10.1006/mpev.2001.1056
573 Morel, J. (1979). *Le campagnol terrestre en Suisse: Biologie et systématique (Mammalia*
574 *Rodentia).* Université de Lausanne.
575 Mouton, A., Mortelliti, A., Grill, A., Sara, M., Kryštufek, B., Juškaitis, R., … Michaux, J. R.
576 (2017). Evolutionary history and species delimitations: a case study of the hazel
577 dormouse, Muscardinus avellanarius. *Conservation Genetics*, *18*(1), 181–196.
578 https://doi.org/10.1007/s10592-016-0892-8
579 Pardiñas, U., Ruelas, D., Bradley, L., Bradley, R., Ordonez, N., Kryštufek, B., … Brito M., J.
580 (2017). Cricetidae (true hamsters, voles, lemmings and new world rats and mice) -
581 Species accounts of Cricetidae. In D. . Wilson, T. E. J. Lacher, & R. A. Mittermeier
582 (Eds.), *Handbook of the Mammals of the World. Volume 7. Rodents II.* (Lynx Edici, pp.
583 280–535). Barcelona.
584 Paupério, J., Herman, J. S., Melo-Ferreira, J., Jaarola, M., Alves, P. C., & Searle, J. B. (2012).
585 Cryptic speciation in the field vole: a multilocus approach confirms three highly
586 divergent lineages in Eurasia. *Molecular Ecology*, *21*(24), 6015–6032.
587 https://doi.org/10.1111/mec.12024
588 Rambaut, A., Suchard, M. A., Xie, D., & Drummond, A. J. (2014). *Tracer v1.6*
589 *http://beast.bio.ed.ac.uk/Tracer*.
590 Rambaut, Andrew. (2012). *FigTree v1.4. http://tree.bio.ed.ac.uk/software/figtree/*.
591 Renaud, S., Dufour, A.-B., Hardouin, E. A., Ledevin, R., & Auffray, J.-C. (2015). Once upon
592 Multivariate Analyses: When They Tell Several Stories about Biological Evolution.
593 *PLOS ONE*, *10*(7), e0132801.
594 Renaud, S., Hardouin, E. A., Quéré, J. P., & Chevret, P. (2017). Morphometric variations at
595 an ecological scale: Seasonal and local variations in feral and commensal house mice.

Mammalian Biology, *87*, 1–12. https://doi.org/10.1016/j.mambio.2017.04.004

Rohlf, F. J. (2010). *Tpsdig v.2. Ver. 2.16: Ecology and Evolution, SUNY at Stony Brook.*

Rohlf, F.James, & Slice, D. (1990). Extensions of the Procrustes Method for the Optimal Superimposition of Landmarks. *Systematic Biology*, *39*(1), 40–59.

Ronquist, F., Teslenko, M., van der Mark, P., Ayres, D. L., Darling, A., Höhna, S., … Huelsenbeck, J. P. (2012). MrBayes 3.2: Efficient Bayesian Phylogenetic Inference and Model Choice Across a Large Model Space. *Systematic Biology*, *61*(3), 539–542. https://doi.org/10.1093/sysbio/sys029

Rozas, J., Ferrer-Mata, A., Sánchez-DelBarrio, J. C., Guirao-Rico, S., Librado, P., Ramos-Onsins, S. E., & Sánchez-Gracia, A. (2017). DnaSP 6: DNA Sequence Polymorphism Analysis of Large Data Sets. *Molecular Biology and Evolution*, *34*(12), 3299–3302. https://doi.org/10.1093/molbev/msx248

Samuels, J. X., & Van Valkenburgh, B. (2009). Craniodental Adaptations for Digging in Extinct Burrowing Beavers. *Journal of Vertebrate Paleontology*, *29*(1), 254–268.

Schlager, S. (2017). Morpho and Rvcg - Shape Analysis in R. In G. Zheng, S. Li, & G. Szekely (Eds.), *Statistical Shape and Deformation Analysis* (pp. 217–256). Academic Press.

Searle, J. B., Kotlík, P., Rambau, R. V, Marková, S., Herman, J. S., & McDevitt, A. D. (2009). The Celtic fringe of Britain: insights from small mammal phylogeography. *Proceedings. Biological Sciences / The Royal Society*, *276*(1677), 4287–4294. https://doi.org/10.1098/rspb.2009.1422

Taberlet, P., Fumagalli, L., Wust-Saucy, A. G., & Cosson, J.-F. (1998). Comparative phylogeography and postglacial colonization routes in Europe. *Mol. Ecol.*, *7*(4), 453–464.

Vallejo, R. M., & González-Cózatl, F. X. (2012). Phylogenetic affinities and species limits within the genus Megadontomys (Rodentia: Cricetidae) based on mitochondrial sequence data. *Journal of Zoological Systematics and Evolutionary Research*, *50*(1), 67–75. https://doi.org/10.1111/j.1439-0469.2011.00634.x

Ventura, J., & Casado-Cruz, M. (2011). Post-weaning ontogeny of the mandible in fossorial water voles: ecological and evolutionary implications. *Acta Zoologica*, *92*(1), 12–20. https://doi.org/10.1111/j.1463-6395.2010.00449.x

Wilson, D. E., & Reeder, D. M. (Eds.). (1993). *Mammals species of the world, a taxonomic and geographic reference. Second edition.* (Smithsonia). Washington.

Wilson, D. E., & Reeder, D. M. (Eds.). (2005). *Mammal Species of the World Third Edition*.

Baltimore: The Johns Hopkins University Press.

Wust-Saucy, A. G. (1998). *Polymorphisme génétique et phylogéographie du campagnol terrestre Arvicola terrestris*. Université de Lausanne.

635

636 **Figure legends**

637

638 Figure 1. Distribution of the ecological forms in the sampled localities (A), genetic network
639 (B) and distribution of the genetic lineages (C).

640

641 Figure 2. Simplified Bayesian phylogeny of *Arvicola* water voles. The support is indicated as
642 follow: Posterior Probability (MrBayes) / Bootstrap Support (PhyMl). The different lineages
643 are indicated on the right side of the phylogeny. For each lineage, the dominant ecotype is
644 indicated in brackets, with its percentage of occurrence based on the number of sequences in
645 the tree attributed to this ecotype.

646

647 Figure 3. Variation of skull centroid size between populations of water voles (above, ventral
648 side; bottom, lateral side). Each dot represents a specimen.

649

650 Figure 4. Skull shape in ventral view. (A). Morphospace corresponding to the first two axes of
651 a PCA on the aligned coordinates. (B). Allometric relationship, represented by the Common
652 Allometric Component in the "GxE" groups (CAC_{GxE}), as a function of centroid size. (C).
653 Visualization of shape changes, as arrows pointing from a first to a second item. From top to
654 bottom: Shape changes along the first PC axis; allometric shape change, from minimum to
655 maximum centroid size along the CAC_{GxE}; change between the mean morphology of *A.*
656 *sapidus* and fossorial lineage 1; change between the mean morphology of aquatic and
657 fossorial forms within lineage 2. (D). Morphospace corresponding to the first two axes of a
658 CVA on the PC axes totaling 95% of shape variance.

659

660 Figure 5. Skull shape in lateral view. (A). Morphospace corresponding to the first two axes of
661 a PCA on the aligned coordinates. (B). Allometric relationship, represented by the Common
662 Allometric Component in the "GxE" groups (CAC_{GxE}), as a function of centroid size. (C).
663 Visualization of shape changes, as arrows pointing from a first to a second item. From top to
664 bottom: Shape changes along the first PC axis; allometric shape change, from minimum to
665 maximum centroid size along the CAC_{GxE}; change between the mean morphology of *A.*
666 *sapidus* and fossorial lineage 1; change between the mean morphology of aquatic and
667 fossorial forms within lineage 2. (D). Morphospace corresponding to the first two axes of a
668 CVA on the PC axes totaling 95% of shape variance.

669

670 **Supporting Information**

671

672 Figure S1. Examples of water vole skulls in ventral and lateral view, with the location of the
673 landmarks (red dots) and sliding semi-landmarks (blue dots along the black lines).

674

675 Figure S2. Phylogenetic tree reconstructed with the cytochrome *b* mitochondrial gene. For the
676 main nodes, the support is indicated as follow: posterior probability (MrBayes) / bootstrap
677 support (PhyMl). The different lineages are indicated on the right side of the phylogeny. The
678 color code of the sequence names represents the ecology: in orange fossorial; in blue aquatic.

679

680 Table S1. Sampling for the genetic study. Abbreviations: JPQ = Jean-Pierre Quéré, JRM =
681 Johan R. Michaux, RGU = Rainer G. Ulrich.

682

683 Table S2. Sampling for the morphometric study.
684 GxE: grouping variable combining genetics and ecology. Nventra/Nlateral: number of skulls
685 measured in ventral/lateral view. Abbreviations: JPQ = Jean-Pierre Quéré; JRM = Johan R.
686 Michaux, CBGP: Centre de Biologie et Gestion des Populations (Baillarguet, Paris), MHN:
687 Muséum d'Histoire Naturelle (Geneva, Switzerland), ULG = Université de Liège (Belgium).

688

689 Alignment S1. Alignments of Cytb sequences used in the present study.

690

691

692 Table 1. K2P distances and standard error between (below the diagonal) and within (on the diagonal)
693 lineages.

	Lineage 1	Lineage2	Lineage 3	Lineage 4	*A. sapidus*	*A. persicus*	Outgroup
Lineage 1	1.3 ± 0.2						
Lineage 2	4.1 ± 0.6	1.2 ± 0.2					
Lineage 3	3.8 ± 0.6	2.9 ± 0.5	0.6 ± 0.2				
Lineage 4	5.1 ± 0.8	4.4 ± 0.7	4.8 ± 0.8	1.6 ± 0.3			
A. sapidus	7.5 ± 1	7.2 ± 0.9	7.6 ± 1	8.1 ± 1.1	0.9 ± 0.2		
A. persicus	9.4 ± 1.2	10.1 ± 1.2	9.8 ± 1.2	9.2 ± 1.1	10 ± 1.2	1.2 ± 0.3	
Outgroup	19.2 ± 1.5	18.5 ± 1.4	18.3 ± 1.5	17.5 ± 1.5	17.8 ± 1.4	19 ± 1.5	17.2 ± 1.4

694

695

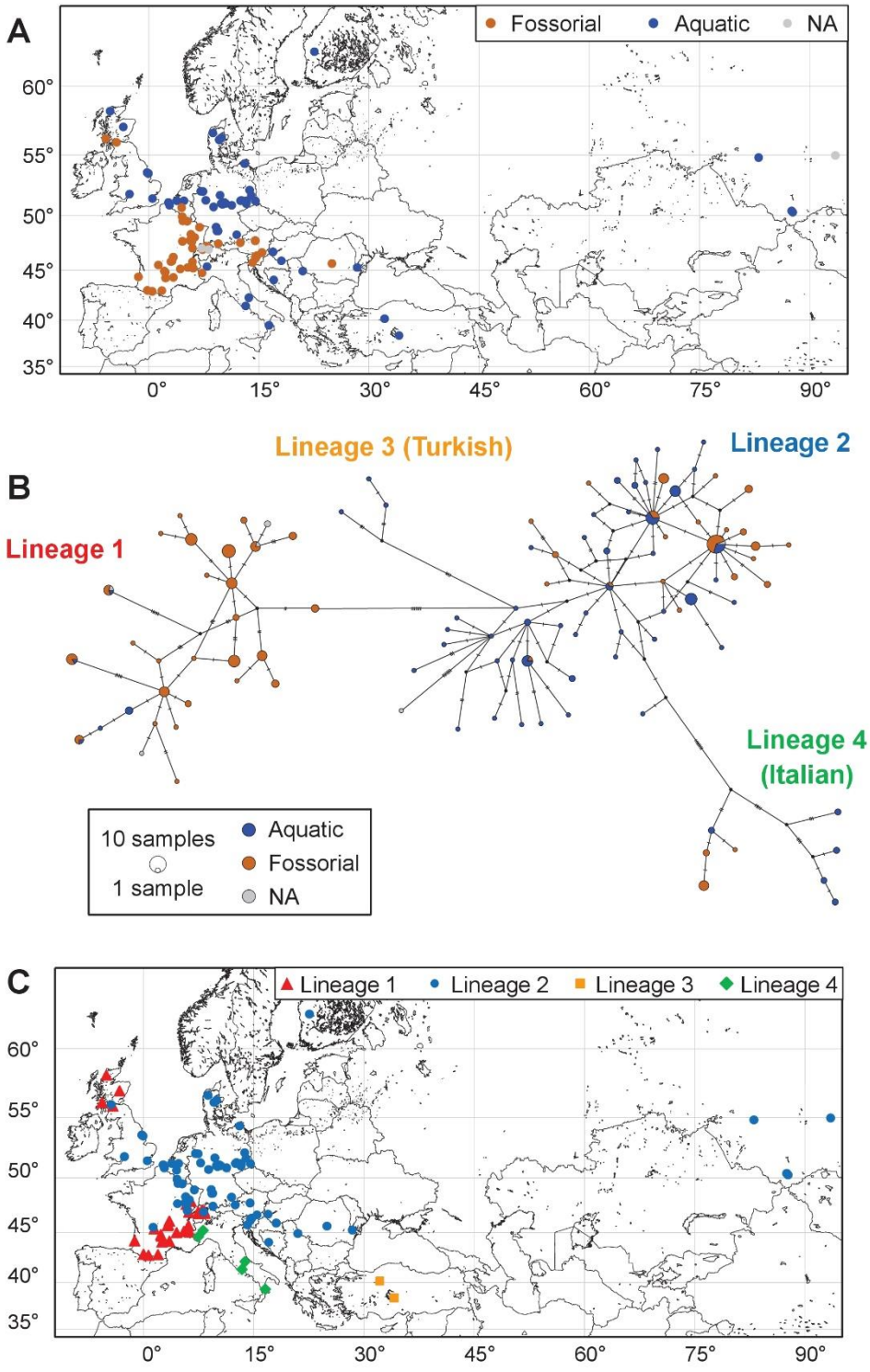
A
Fossorial
Aquatic
NA
60°
55°
50°
45°
40°
35°
0°
15°
30°
45°
60°
75°
90°
B
Lineage 3 (Turkish)
Lineage 2
Lineage 1
Lineage 4
(Italian)
10 samples
1 sample
Aquatic
Fossorial
NA
C
Lineage 1
Lineage 2
Lineage 3
Lineage 4
60°
55°
50°
45°
40°
35°
0°
15°
30°
45°
60°
75°
90°

696

697

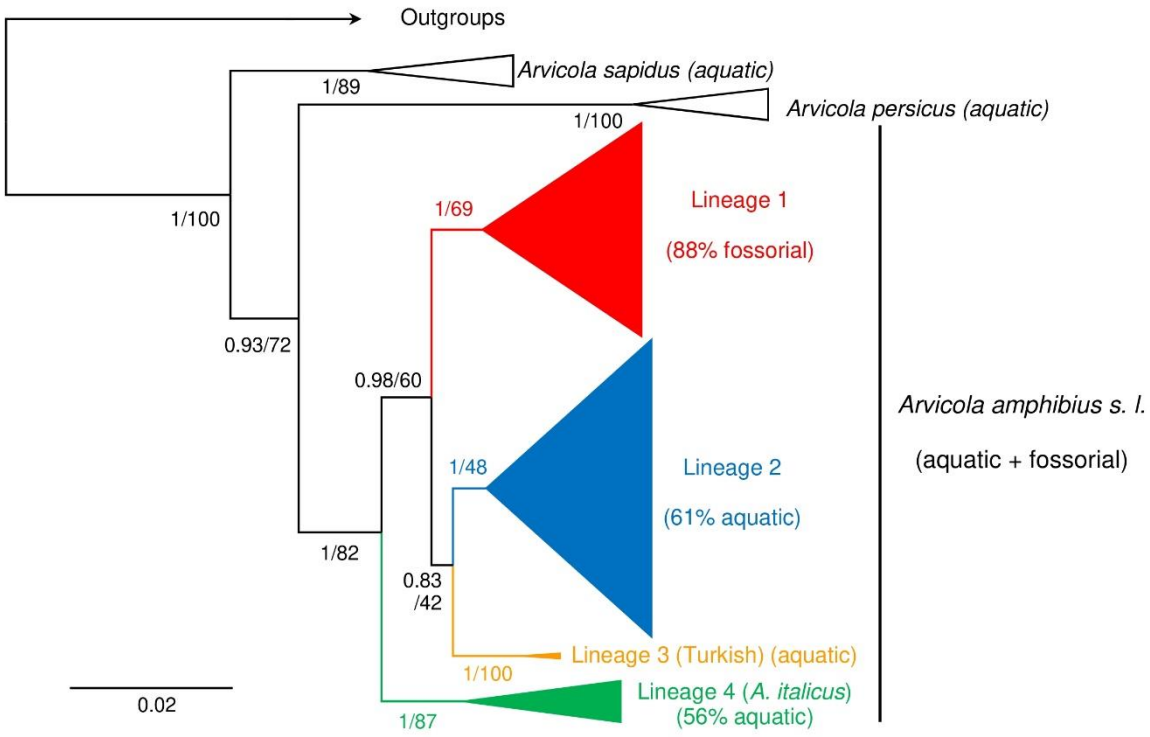
Outgroups
Arvicola sapidus (aquatic)
1/89
Arvicola persicus (aquatic)
1/100
1/100
1/69
Lineage 1
(88% fossorial)
0.93/72
0.98/60
Arvicola amphibius s. l.
(aquatic + fossorial)
1/48
Lineage 2
(61% aquatic)
1/82
0.83
/42
Lineage 3 (Turkish) (aquatic)
1/100
0.02
Lineage 4 (A. italicus)
(56% aquatic)
1/87

698

699

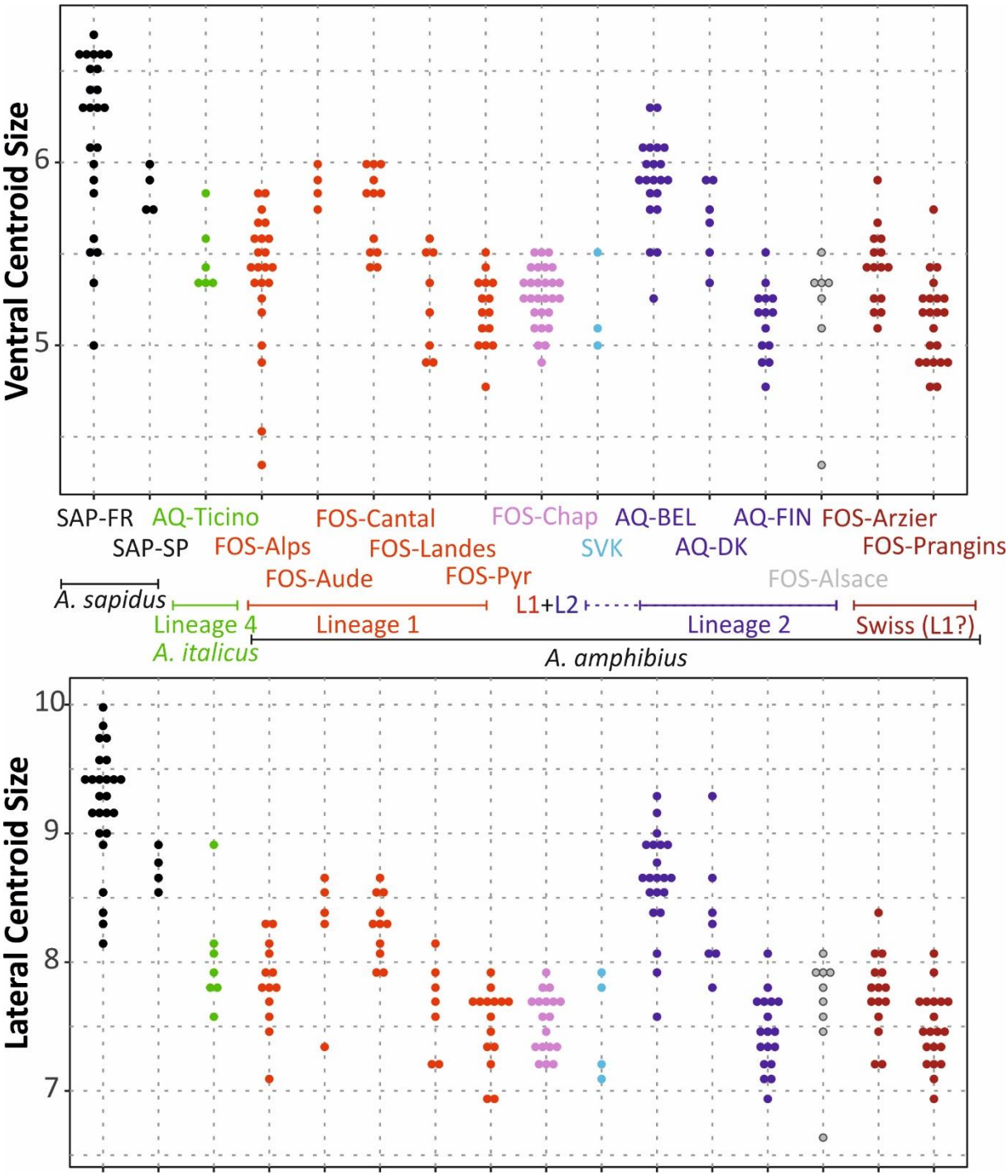
Ventral Centroid Size
6
5
SAP-FR
SAP-SP
AQ-Ticino
FOS-Alps
FOS-Cantal
FOS-Landes
FOS-Aude
FOS-Pyr
FOS-Chap
SVK
AQ-BEL
AQ-DK
AQ-FIN
FOS-Alsace
FOS-Arzier
FOS-Prangins
A. sapidus
Lineage 4
A. italicus
Lineage 1
L1+L2
Lineage 2
Swiss (L1?)
A. amphibius
Lateral Centroid Size
10
9
8
7

700

701

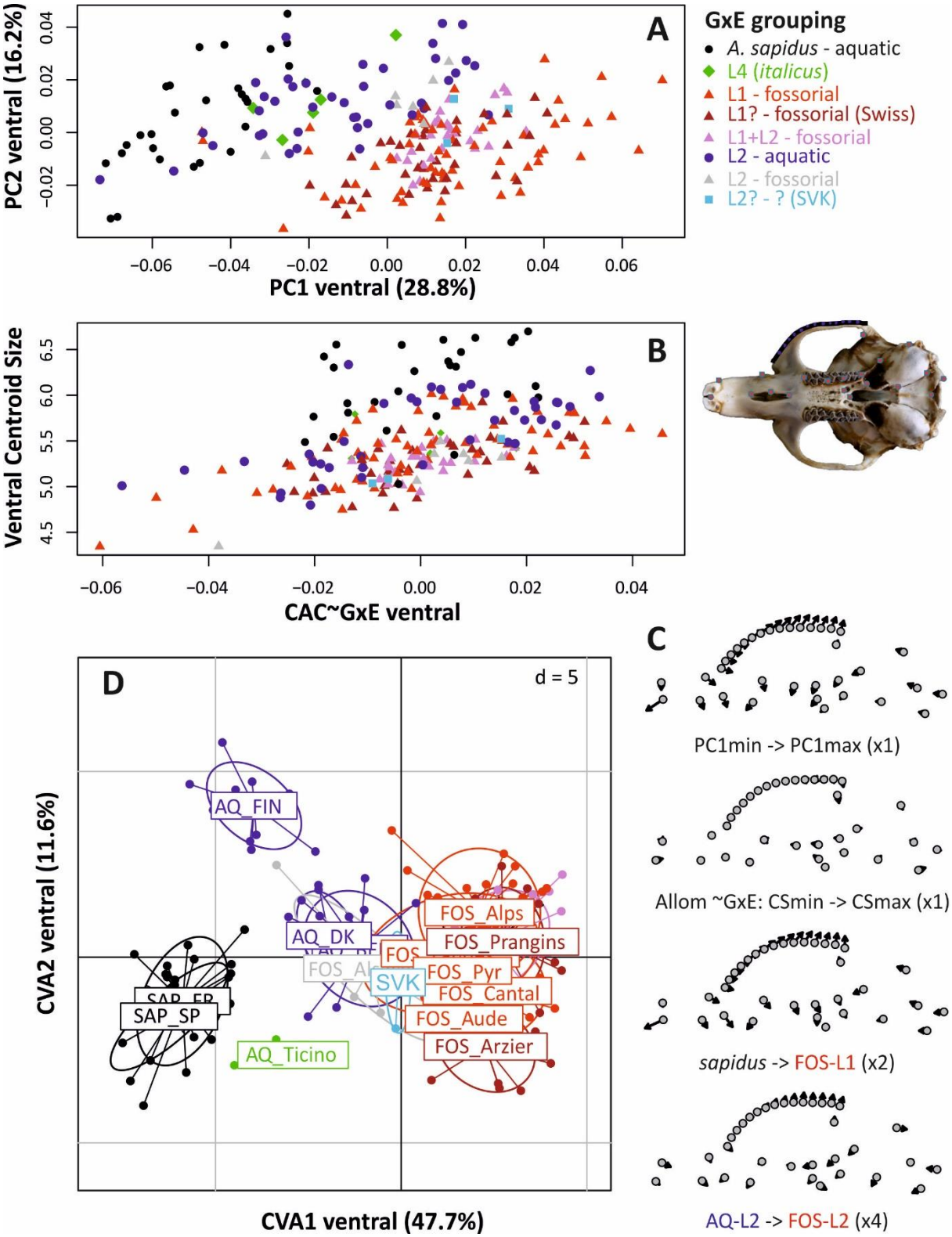
A
PC2 ventral (16.2%)
PC1 ventral (28.8%)
GxE grouping
A. sapidus - aquatic
L4 (italicus)
L1 - fossorial
L1? - fossorial (Swiss)
L1+L2 - fossorial
L2 - aquatic
L2 - fossorial
L2? - ? (SVK)
B
Ventral Centroid Size
CAC~GxE ventral
C
PC1min -> PC1max (x1)
Allom ~GxE: CSmin -> CSmax (x1)
sapidus -> FOS-L1 (x2)
AQ-L2 -> FOS-L2 (x4)
D
d = 5
CVA2 ventral (11.6%)
CVA1 ventral (47.7%)
AQ_FIN
AQ_DK
AQ_Ticino
SAP_SP
SVK
FOS_Alps
FOS_Prangins
FOS_Pyr
FOS_Cantal
FOS_Aude
FOS_Arzier

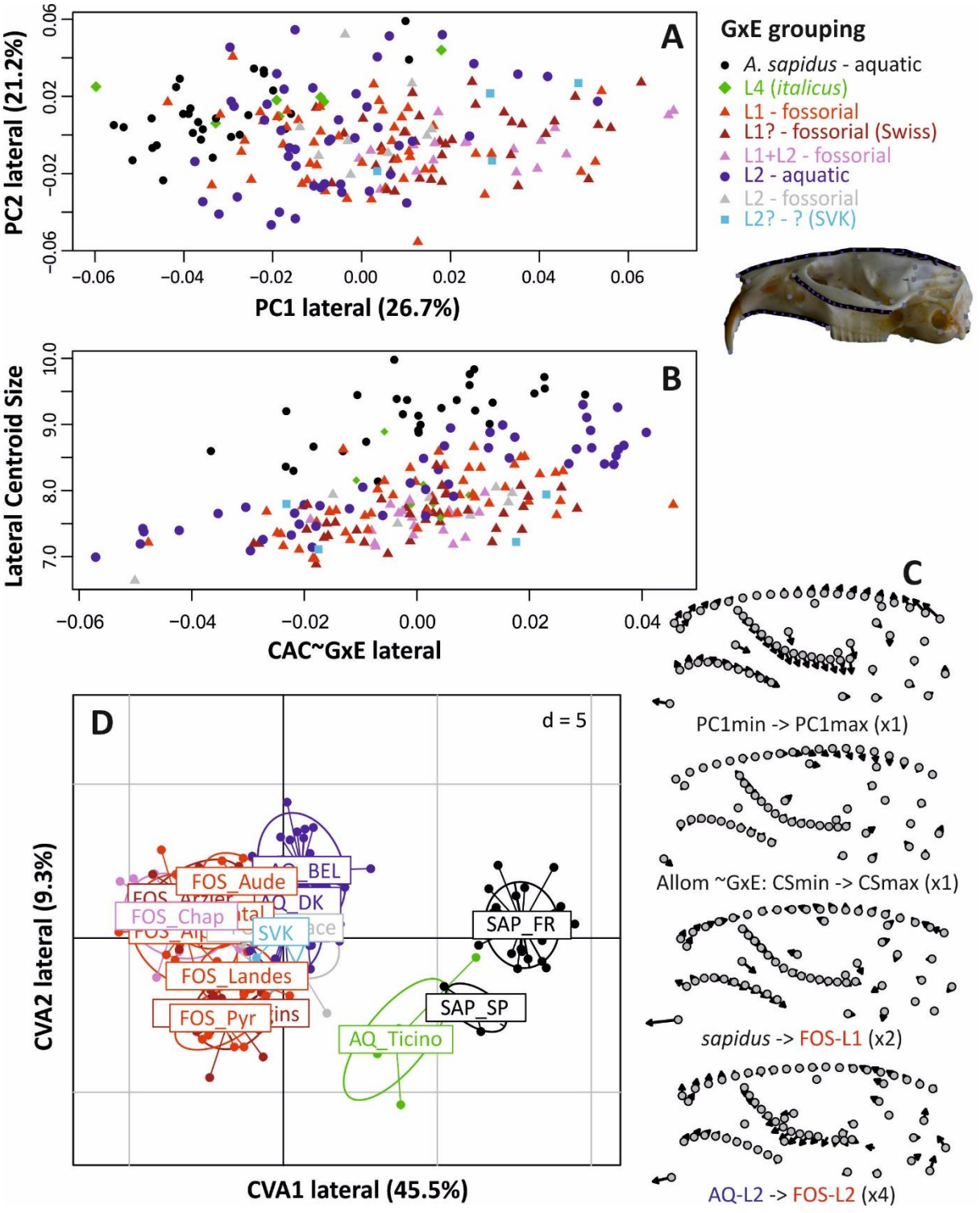
A
PC2 lateral (21.2%)
PC1 lateral (26.7%)
GxE grouping
A. sapidus - aquatic
L4 (italicus)
L1 - fossorial
L1? - fossorial (Swiss)
L1+L2 - fossorial
L2 - aquatic
L2 - fossorial
L2? - ? (SVK)
B
Lateral Centroid Size
CAC~GxE lateral
C
PC1min -> PC1max (x1)
Allom ~GxE: CSmin -> CSmax (x1)
sapidus -> FOS-L1 (x2)
AQ-L2 -> FOS-L2 (x4)
D
d = 5
CVA2 lateral (9.3%)
CVA1 lateral (45.5%)
FOS_Aude
FOS_Chap
FOS_Landes
FOS_Pyr
SVK
SAP_FR
SAP_SP
AQ_Ticino

704